J Electr Eng Technol.2018; 13(1): 152-159
http://doi.org/10.5370/JEET.2018.13.1.152

ISSN(Print) 1975-0102
ISSN(Online) 2093-7423

A Novel Cost-Effective Two-Level Inverter with Combined Use of Thyristors and IGBTs

Dezhi Chen*, Wenliang Zhao and Byung-il Kwon†**

Abstract – In this paper, a novel topology of two-level voltage-type inverter is proposed. The proposed inverter has three bridge arms while each bridge is made up of two thyristors, one IGBT and four diodes. Thyristors complete the phase positioning of the inverter, IGBT completes the modulation of different modulation modes such as SPWM, SVPWM, and SHPWM, and the diodes complete the commutation of the bridge arms. Compared to the traditional voltage-type inverter with six IGBTs, the proposed voltage-type inverter using three IGBTs can achieve the same function with highly reduced cost. The principle of the proposed two-level inverter is explained in detail. The simulation and experiment results demonstrate the performance and effectiveness of the proposed inverter-type inverter.

Keywords: Cost, diode, IGBT, inverter-type inverter, Thyristor

1. Introduction

In recent years, the voltage-type inverters have been widely applied in numerous applications such as the AC-DC variable frequency speed regulation system, induction heating, uninterruptable power supplies, and electric power system. However, with the increasing use of the power electronic devices, the voltage grade, stability, and cost problems of the inverters cannot be ignored. Accordingly, the domestic and foreign scholars have conducted a lot of research work [1-5].

The research on the multilevel inverter structure and intelligent control algorithm have been investigated in [6] and [7], which improves the system voltage level and performance. The topology of modular multilevel converter (MMC) is adopted in [8] and [9] in order to increase the voltage level of inverter and reduce the capacity of IGBT, making IGBT widely used in the field of HVDC transmission, and the inverter of HVDC is discussed in depth. In [10] and [11], the multilevel inverter topology of the IGBT reverse series is proposed. Four quadrant operation and simplify control of the system are accomplished using this structure. A converter of AC-AC is proposed in [12], which eliminates the intermediate DC link. The AC-AC power conversion is achieved in the converter, which the rectifier part uses six IGBTs and the inverter uses six IGBTs. Overall, the topologies of multilevel, matrix converter, and MMC are adopted by domestic and overseas scholars in order to increase the voltage level and the performance of the system, making the power device of small capacity applied to high voltage and high power system.

Obviously, the IGBTs are one of the major components of the inverters which essentially determine the complexity, cost and efficiency of the system. However, the use of a large number of IGBTs not only contributes to promising superiority in terms of voltage blocking capability and switching frequency, but also increase the cost of the system. In [13], the gate turn-off thyristors and IGBT are utilized to constitute the active power filter to save the cost. In [14], the MMC new topology structure with thyristors and IGBT is proposed to reduce the switch loss and system costs. In [15], the method by using reduced transistors for voltage source inverter has been introduced but limited to preliminarily theoretical analysis and simulation.

In this paper, a novel cost-effective two-level voltage-type inverter with six thyristors, three IGBTs, and two diodes is proposed based on a traditional inverter with six IGBTs. The key of the proposed inverter is the use of less inexpensive thyristors replacing the expensive IGBTs, but realizing the similar features compared to the conventional one. The topology, principle, energy flow mode, and thyristor switch timing of the proposed two-level inverter are first discussed in detail. Then the simulation and experiment platform for the proposed two-level inverter based on sinusoidal pulse width modulation (SPWM) are established. As a result, the simulation and experiment results verify the performance and effectiveness of the proposed inverter-type inverter.

2. Inverter Topology and Operating Principle

Fig. 1 shows the traditional structure of the two-level

† Corresponding Author: Department of Electronic Systems Engineering, Hanyang University, Korea. (bikwon@hanyang.ac.kr)
* School of Electrical Engineering, Shenyang University of Technology, China. (chendezhi@sut.edu.cn)
** School of Electrical Engineering, Shandong University, China. (wlzhao@sdu.edu.cn)
Received: August 26, 2016; Accepted: August 14, 2017

Table 1. Electric devices and cost estimation

Item	Conventional	Proposed
IGBT	6	3
Diode	6	12
Thyristor	0	6
Cost	104 $	33 $

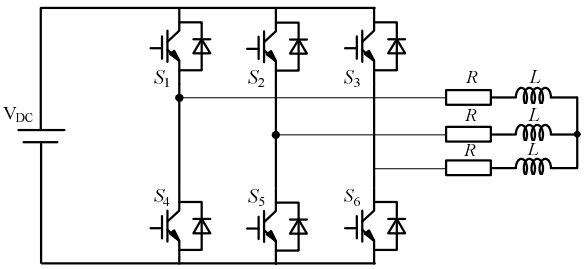

Fig. 1. Topology of the traditional two-level inverter

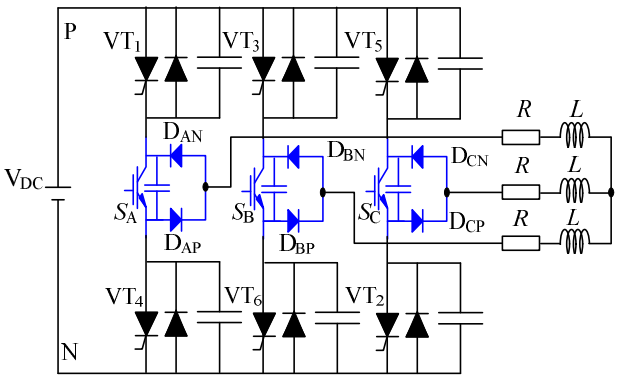

Fig. 2. Topology of the proposed two-level inverter

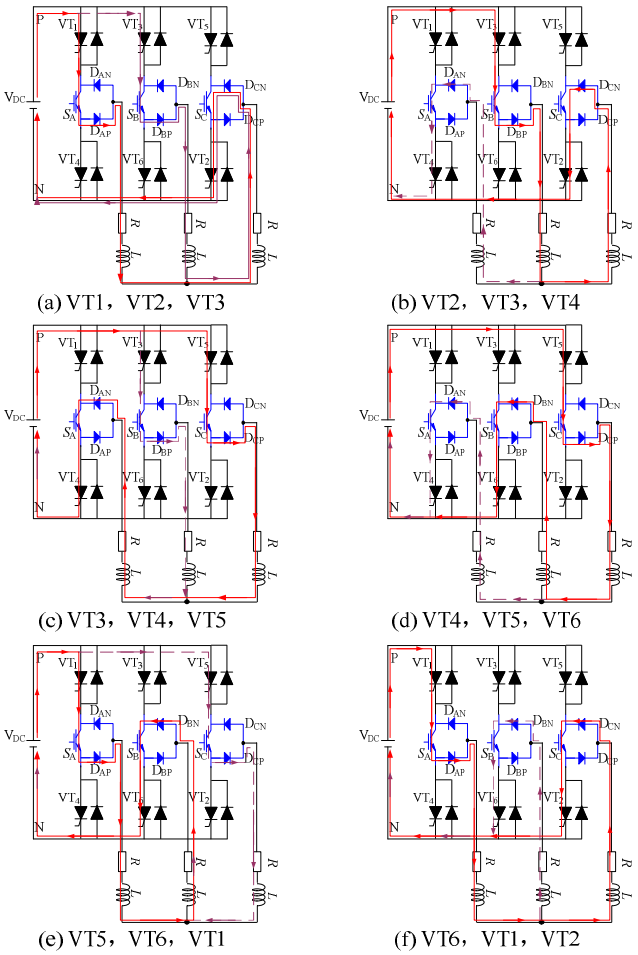

Fig. 3. Energy transfer model of new-type two level inverter

voltage-type inverter, while Fig. 2 shows the topology of the proposed two-level voltage-type inverter. The utilization of electric switches and estimated cost are listed in Table 1.

From Fig. 1, it can be seen that the traditional two-level voltage-type inverter is mainly made up of six IGBTs (S_1, S_2, S_3, S_4, S_5 and S_6), and define the switching function S; when S = 1, the upper bridge arm open, the lower bridge arm off; when S = 0, the upper bridge arm off, the lower bridge arm open. Therefore, we get eight kinds of switching inverters (000 ~ 111). At the same time, there are three IGBT in the conduction state.

In Fig. 2, the main parts of the proposed two-level inverter are six thyristors (VT1, VT2, VT3, VT4, VT5 and VT6), three IGBTs (S_A, S_B and S_C), and twelve diodes (D_{AN}, D_{BN}, D_{CN}, D_{AP}, D_{BP}, etc.). Combined with corresponding control algorithms, the proposed voltage-type inverter can achieve the identical functions of the traditional two-level inverter which is shown in Fig. 1 [16].

2.1 Energy transfer model

The output waveforms of the novel inverter with voltage-phase angle 120° between three phases voltage using the thyristors, realize all kinds of modulation algorithm using IGBTs and complete converter using diodes. Fig. 3 is the six kinds of energy transfer mode of the novel two-level inverter under different switch state.

(1) As shown in Fig. 3 (a) and Table 1（Switch signal is 110）, the thyristors VT1, VT2, VT3 of the novel two-level inverter work. The energy transfer path of the system is the V_{DC} positive terminal to VT1 - S_A - D_{AP} - A phase load - B phase load - D_{CN} -S_C - VT2 - V_{DC} negative terminal; V_{DC} positive terminal - VT3 - S_B - D_{BP} - B phase load - C phase load -D_{CN}-S_C-VT2-V_{DC} negative terminal.

(2) As shown in Fig. 3 (b) and Table 1（Switch signal is 010）, the thyristors VT2, VT3, VT4 of the novel two-level inverter work. The energy transfer path of the system is the V_{DC} positive end to VT3 - S_B - D_{BP} - B phase load - C phase load - D_{CN} - S_C- VT2 - V_{DC} negative terminal; V_{DC} positive terminal - VT3 - S_B - D_{BP} - B phase load - A phase load - D_{AN} - S_A - VT4 - V_{DC} negative terminal.

(3) As shown in Fig. 3 (c) and Table 1（Switch signal is 011), the thyristors VT3, VT4, VT5 of the novel two-level inverter work. The energy transfer path of the system is the VDC positive terminal to VT3 - S_B - D_{BP} - B phase load - A

phase load - D_{SA}- VT4 - V_{DC} negative terminal; V_{DC} positive terminal - VT5 - S_C - D_{CP} - C phase load - A phase load - D_{AN} - S_A - VT4 - V_{DC} negative terminal.

(4) As shown in Fig. 3 (d) and Table 1 (Switch signal is 001, the thyristors VT4, VT5, VT6 of the novel two-level inverter work. The energy transfer path of the system is the V_{DC} positive terminal to VT5 - S_C - D_{CP} - C phase load - B phase load – D_{BN} - S_B- VT6 - V_{DC} negative terminal; VDC positive terminal - VT5 - S_C - DCP - C phase load - A phase load - DAN - S_A - VT4 - VDC negative terminal.

(5) As shown in Fig. 3 (e) and Table 1 (Switch signal is 101, the thyristors VT5, VT6, VT1 of the novel two-level inverter work. The energy transfer path of the system is the V_{DC} positive terminal to VT5 - S_C - D_{CP} - C phase load - B phase load – D_{BN} - S_B- VT6 - V_{DC} negative terminal; V_{DC} positive terminal – VT1 - S_A - D_{AP} - A phase load - B phase load - D_{BN} - S_B –VT6 -V_{DC} negative terminal.

(6) As shown in Fig. 3 (f) and Table 1 (Switch signal is 100, the thyristors VT6, Vt1, VT2 of the novel two-level inverter work. The energy transfer path of the system is the V_{DC} positive terminal to VT1 - S_A - D_{AP}- A phase load - B phase load – D_{BN} - S_B - VT6 - V_{DC} negative terminal; V_{DC} positive terminal – VT1 - S_A - D_{AP} - A phase load - C phase load - D_{CN} - S_C – VT2 - V_{DC} negative terminal.

2.2 Switch state

According to a cycle of energy transfer mode as shown in Fig. 3, the table of switch time series and switch state of the novel two-level inverter can be got. Fig. 4 is the sequence diagram of the thyristor VT1 to VT6 and the switch of S_A- S_C. Here we set the value of the upper bridge-arm (VT1,VT3,VT5,S_A,S_B,S_C) as 1 and the lower bridge-arm(VT2,VT4,VT6,S_A,S_B,S_C) as 0, the switch state's table of novel two-level inverter can be built, as shown in Table 2.

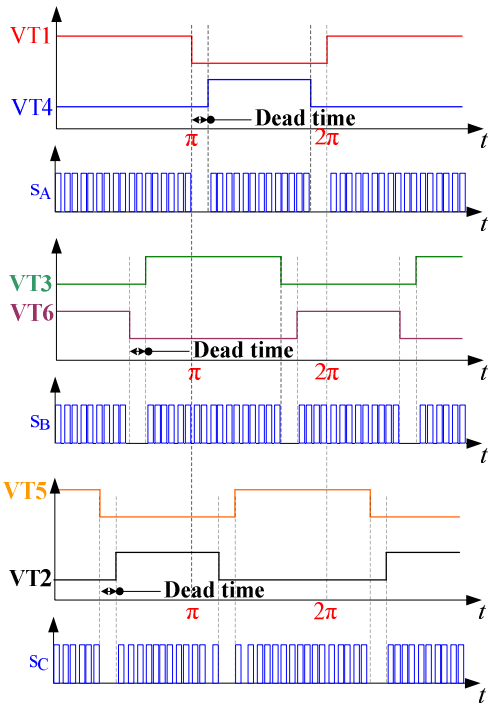

Fig. 4. Switch time series of novel two-level inverter

As shown in Fig. 4: have there is a difference of 180 degrees between thyristors VT1 and VT4; VT3 and VT6; VT2 and VT5respectively, and a difference between 120 degrees between VT1 and VT3, VT5. IGBT S_A, S_B, S_C output sinusoidal pulse width modulation wave.

2.3 Analysis of drive signal for IGBT

Generally, there are the symmetrical rule sampling method, the asymmetry rule sampling method and the equivalent area method in the SPWM's modulation. The asymmetry rule sampling method is adopted for the IGBT SVPWM modulation in the novel two-level inverter. The schematic diagram has been shown in Fig. 5, asymmetry rule sampling method has sampling twice in each carrier cycle and the sampling location is located at the vertex positions and the end-point positions of triangular wave.

According to similar triangle principle,

$$\begin{cases} \dfrac{\delta'}{T_c/2} = \dfrac{1+a\sin\omega t_A}{2} \\ \dfrac{\delta}{T_c/2} = \dfrac{1+a\sin\omega t_B}{2} \end{cases} \quad (1)$$

Table 2. Switch state of novel two-level inverter

Switch state	Switch signal			Output line voltage		
				V_{AB}	V_{BC}	V_{CA}
1	0	0	0	0	0	0
2	0	0	1	0	- V_{DC}	V_{DC}
3	0	1	0	- V_{DC}	V_{DC}	0
4	0	1	1	- V_{DC}	0	V_{DC}
5	1	0	0	V_{DC}	0	- V_{DC}
6	1	0	1	V_{DC}	- V_{DC}	0
7	1	1	0	0	V_{DC}	- V_{DC}
8	1	1	1	0	0	0

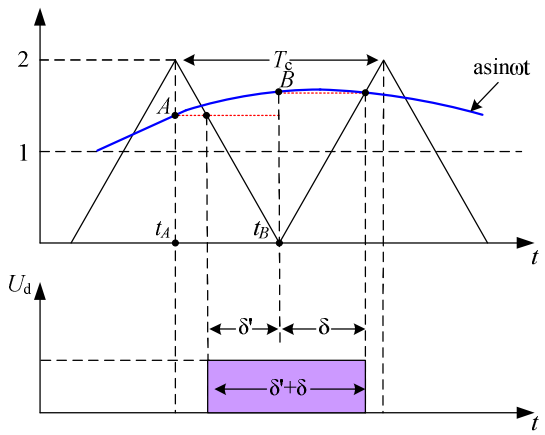

Fig. 5. The principle diagram of the asymmetry rule sampling method

Then

$$\begin{cases} \delta' = \dfrac{T_c\left(1+a\sin\omega t_A\right)}{4} \\ \delta = \dfrac{T_c\left(1+a\sin\omega t_B\right)}{4} \end{cases} \tag{2}$$

Then

$$\delta' + \delta = \frac{T_c\left(2+a\sin\omega t_A + a\sin\omega t_B\right)}{4} \tag{3}$$

The asymmetry rule sampling method of SPWM's modulation can be achieved by bring (3) into the compared register of DSP28335 of TI Company.

$$\begin{cases} EPWM1\mathrm{Re}gs.CMPx = EPWM1\mathrm{Re}gs.TBPRD * \\ \qquad \left(0.5-0.25\left(a\sin\omega t_A + a\sin\omega t_B\right)\right) \\ EPWM2\mathrm{Re}gs.CMPx = EPWM2\mathrm{Re}gs.TBPRD * \\ \qquad \left(0.5-0.25\left(a\sin(\omega t_A - \frac{2\pi}{3}) + a\sin(\omega t_B - \frac{2\pi}{3})\right)\right) \\ EPWM3\mathrm{Re}gs.CMPx = EPWM3\mathrm{Re}gs.TBPRD * \\ \qquad \left(0.5-0.25\left(a\sin(\omega t_A + \frac{2\pi}{3}) + a\sin(\omega t_B + \frac{2\pi}{3})\right)\right) \end{cases} \tag{4}$$

Table 3. Basic parameter of new-type two level inverter

Item	Value	Item	Value
DC source	80V	*R*/*L* load	5Ω/2.5mH
Switching frequency	2kHz	Dead-time	60us
Modulation factor	0.8	Output frequency	50Hz

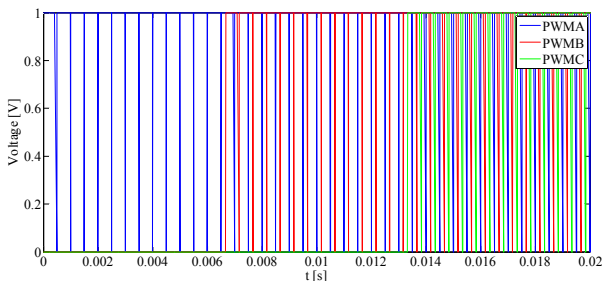

(a) Switch signal of SPWM

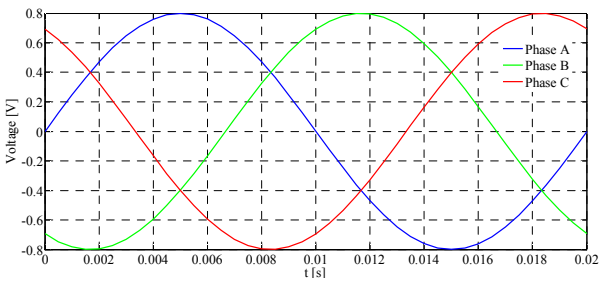

(b) Modulation signal of SPWM

Fig. 6. Signal of SPWM

Fig. 6 (a) is switch signal of SPWM. Fig. 6 (b) is switch signal of SPWM after low-pass filter.

It can be seen from Fig .6, the SPWM waveform after modulation has a good sine degree which can be used for the simulation and experiment. Table 3 shows the basic parameter of new-type two level inverter.

3. Simulation Results

The simulation model can be established based on basic parameters of the novel two-level inverter as shown in table 2. Fig. 7 is the output waveform of the VT1 to VT6 and the IGBT drive. Fig.8 is the waveform at both ends of the VT1 to VT6 and IGBT. Fig. 9 is the output voltage waveform of the inverter. Fig.10 is the output current waveform of the inverter.

It can be seen from Fig. 7 and Fig. 8, the same thyristor of bridge arm (VT1 and VT2, VT3 and VT4, VT5 and VT6) phase different is 180°; different thyristor of bridge arm phase different is 120°. Meanwhile, the output voltage

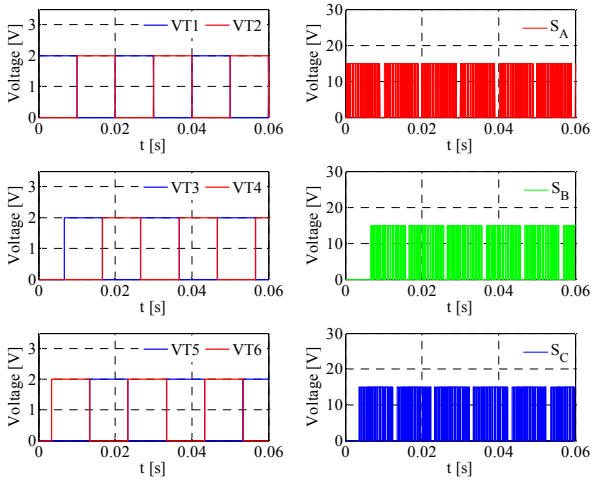

Fig. 7. Waveform of drive for thyristor and IGBT

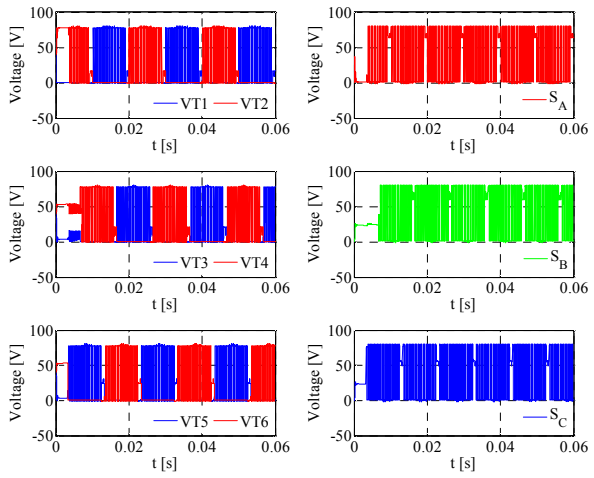

Fig. 8. Voltage of thyristor and IGBT

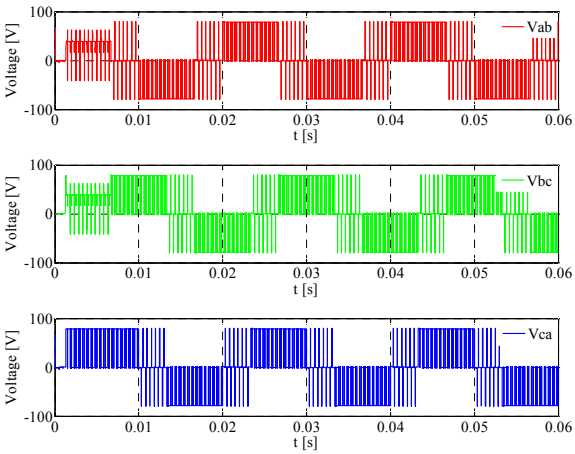

Fig. 9. Output voltage of inverter

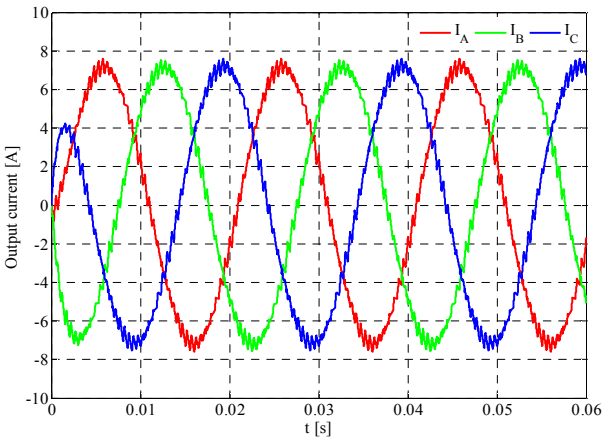

Fig. 10. Output current of inverter

per phase of IGBT (S_A, S_B, S_C) phase different is 120°. The output peak voltage of thyristor and IGBT is 80V, which preliminary verify the accuracy of the proposed scheme.

It can be seen from Fig. 9, the output line voltage of inverter electrical angle different is 120°, and the amplitude voltage is 80V. As can be seen from Fig. 10, the output current of inverter exhibits sine waveforms, validating the correctness of the proposed scheme.

4. Experiment Verification

The novel two-level inverter experimental system is built according to the Table 3 which is shown in Fig. 11, it includes thyristor drive, IGBT drive, DSP board, oscilloscope, power analyzer, DC power supply, and RL load etc.

Some corresponding experiment research can be conducted. The waveforms of phase A, phase B and phase C outputted through DSP are shown in Fig. 12, Fig. 13 and Fig. 14. Fig. 15 shows the three-phase waveform of IGBT outputted through DSP. Fig.16 is the three-phase

(a) Thyristor of on the bridge arm

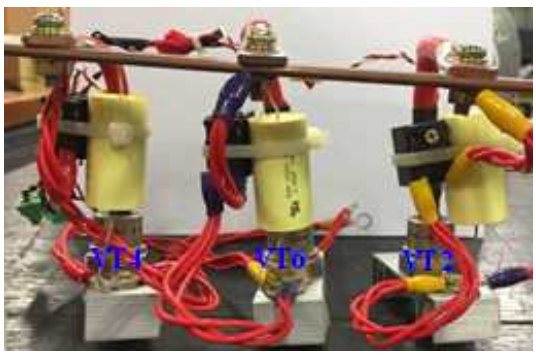

(b) Thyristor of under the bridge arm

(c) Converter diodes of IGBT

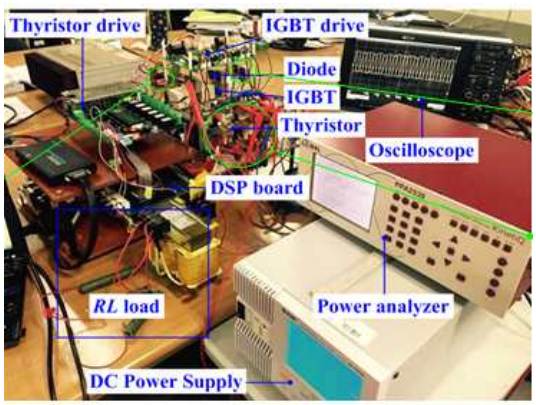

(d) Experimental system setup

Fig. 11. Experiment system

waveform of upper bridge arm switch's thyristor. The three-phase waveform of thyristor's driver is shown in Fig. 17. The output waveform of phase A, phase B and phase C

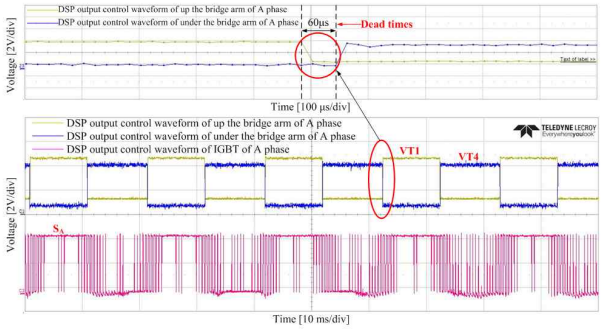

Fig. 12. DSP output waveform of phase A

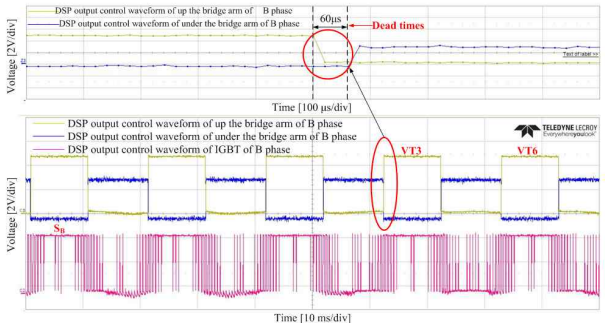

Fig. 13. DSP output waveform of phase B

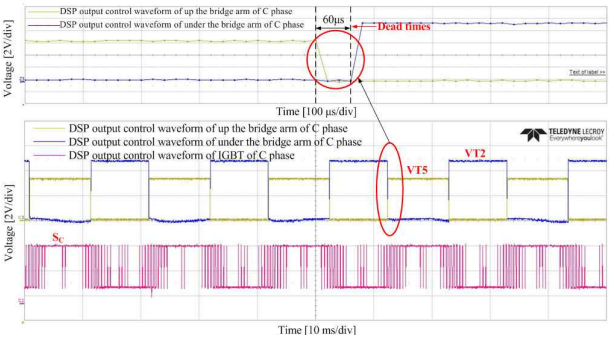

Fig. 14. DSP output waveform of phase C

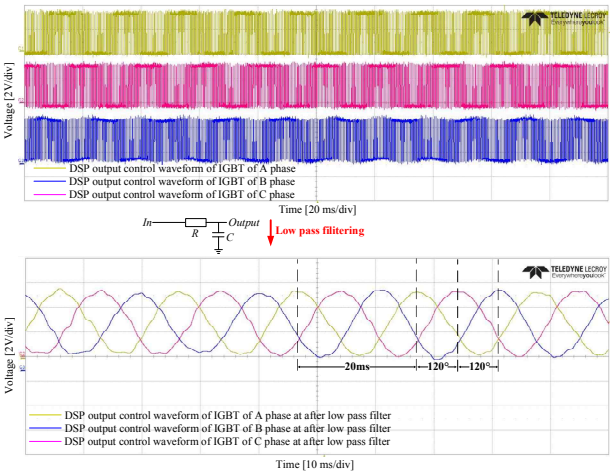

Fig. 15. DSP output waveform of three phase IGBT

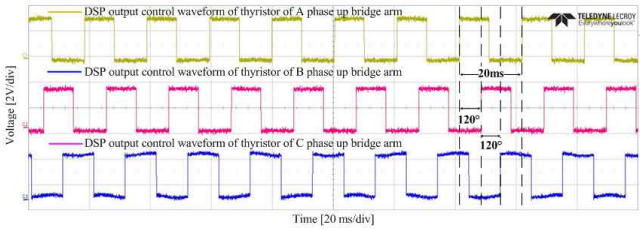

Fig. 16. DSP output waveform of three phase up bridge arm thyristor

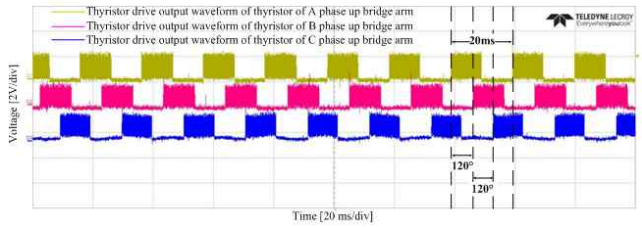

(a) Upper bridge arm

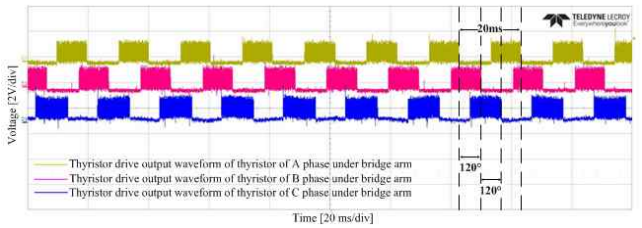

(b) Lower bridge arm

Fig. 17. Thyristor drive output waveform of three phase bridge arm

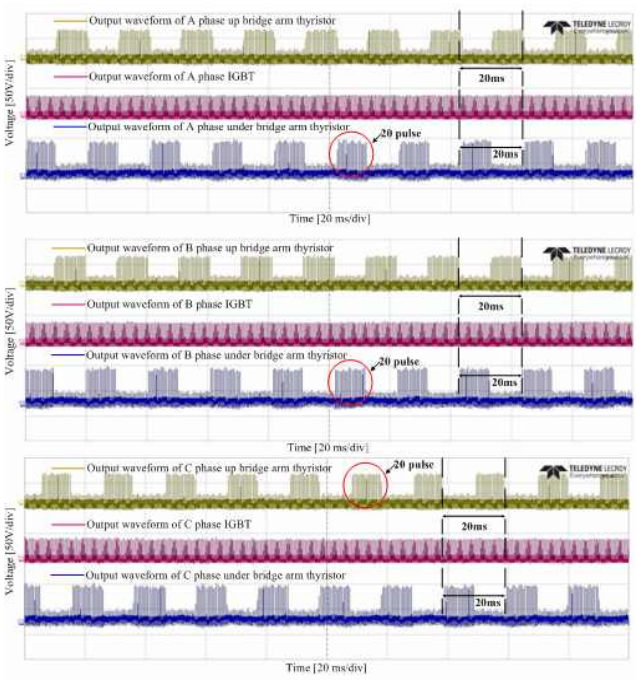

Fig. 18. Output voltage of three phase

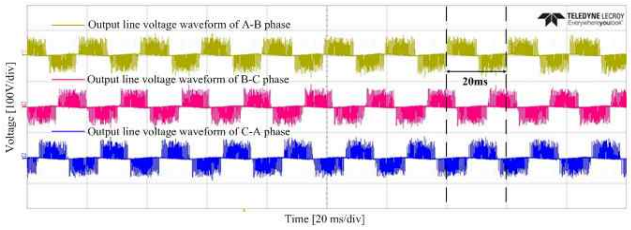

Fig. 19. Output line voltage of three phase

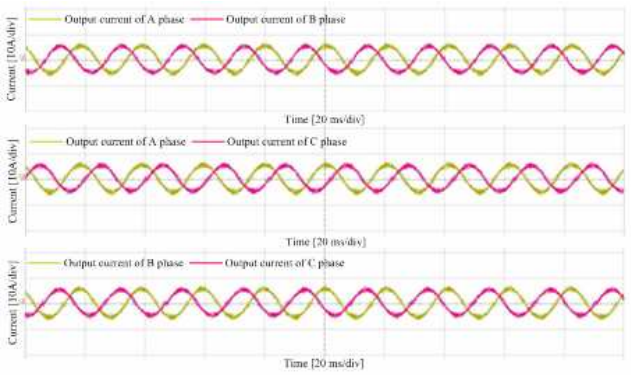

Fig. 20. Output current of inverter

are shown in Fig. 18. The output waveform of three-phase line voltage is shown in Fig. 19. The output waveform of three-phase current is shown in Fig. 20.

From Fig. 12 to Fig. 14, it can be seen that the drive signal difference of thyristors on the same bridge arm is 180°.

In Fig. 15, the amplitude of the IGBT drive signal in three bridge arms is 3V. And after the low pass filter, the output waveform is the sine wave, and the phase difference is 120° with each other.

In Fig. 16, the signal cycle of the upper bridge arm is 20ms, and the phase difference is 120°. From the Fig. 17 and Fig. 18, it can be seen that the phase difference between the upper and lower bridge arms is 120°. The output frequency is 50Hz. The same bridge arm of the thyristors phase difference is 120°. From Fig. 19, it can be seen the output line voltage frequency is 50Hz. The phase angle between three phases is 120°. In Fig. 20, the phase angle of two phase current waveform is 120°, and the sine degree is better.

5. Conclusion

In this paper, a novel cost-effective two-level voltage-type inverter with 6 thyristors, 3 IGBTs, and 12 diodes has been proposed with experimental verification. The energy transfer mode, switching time sequence, switching state, and SPWM modulation method of IGBTs were first analyzed in detail. Then the simulation and experiment platform for the proposed inverter were built and the simulation and experiments were carried out. As a result, the simulation and experimental results have validated the performance and effectiveness of the proposed inverter. Therefore, the proposed voltage-type inverter with combined use of thyristors and IGBTs with low cost has great competitiveness in applications of the cascade multilevel inverter and the matrix type inverter.

Acknowledgements

This work was supported by the research fund of Hanyang University (HY-2014-P).

References

[1] J. J. Patel, A. M. Kubavat, and M. B. Jhala. "Speed control of a three phase induction motor using PWM inverter," *International Journal of Engineering Development and Research*. vol. 2, no. 1, pp. 503-507, 2014.

[2] Chen D, Kwon B, Bai B. "Selection of IGBTs for controlling rectifier and inverter based upon a novel analytical approach for loss calculation," *2015 9th International Conference on Power Electronics and ECCE Asia (ICPE-ECCE Asia)*, pp. 1109-1115, 2015.

[3] Peralta J, Saad H, et al. "Detailed and averaged models for a 401-level MMC–HVDC system," *IEEE Transactions on Power Delivery*. vol. 27, no. 3, pp. 1501-1508, 2012.

[4] N. Mohan, W. P. Robbin and T. Undeland, "Power Electronic: Converters, Applications, and Design," 2nd ed., New York: Wiley, 1995.

[5] R. Dixit, B. Singh et al., "Adjustable Speed Drives: Review on Different Inverter Topologies," *International Journal of Reviews in Computing*, vol. 09, pp. 54-66, 2012.

[6] Alepuz S, Busquets-Monge S, Bordonau J, et al. Interfacing renewable energy sources to the utility grid using a three-level inverter. *IEEE Transactions on Industrial Electronics*. vol. 53, no. 5, pp. 1505-1511, 2006.

[7] C. Newton and M. Sumner "Neutral point control for multi-level inverters: theory, design and operational limitations," in Proc. *IEEE Ind. Appli. Society Annual Meeting*, vol. 2, pp. 1336-1343, Oct 1997.

[8] Saad H, Peralta J, Dennetiere S, et al. "Dynamic averaged and simplified models for MMC-based HVDC transmission systems," *IEEE Transactions on Power Delivery*. vol. 28, no. 3, pp. 1723-1730, 2013.

[9] Bhesaniya M, Shukla A. "Norton Equivalent Modeling of Current Source MMC and Its Use for Dynamic Studies of Back-to-Back Converter System," *IEEE Transactions on Power Delivery*. vol. 32, no. 4, pp. 1935-1944, 2016.

[10] L. Wei, T.A. Lipo, "A novel matrix converter topology with simple commutation," *Proc. of IAS'01*, vol. 3, pp. 1749-1754, 2001.
[11] L. Wei, T. A. Lipo, and H. Chan, "Matrix converter topologies with reduced number of switches," *Proceedings of IEEE PESC'02*, vol. 1, pp. 57-63, 2002.
[12] Kim S, Sul S K, Lipo T A, "AC/AC power conversion based on matrix converter topology with unidirectional switches," *IEEE Transactions on Industry Applications*. vol. 36, no. 1, pp. 139-145, 2000.
[13] Won-Il Choi, Chang-Pyo Hong, and Dong-Hyun Lee, "A common-mode voltage reduction PWM method for three-phase unidirectional rectifier," *IPEMC-ECCE Asia 2016*, pp. 2237-2242.
[14] Dixon J, Valle Y D, Orchard M, et al. "A full compensating system for general loads, based on a combination of thyristor binary compensator, and a PWM-IGBT active power filter," *IEEE Transactions on Industrial Electronics*, vol. 50, no. 5, pp. 982-989, 2003.
[15] S. M. Sajjad Hossain Rafin, T. A. Lipo and Byung-il Kwon, "A novel topology for a voltage source inverter with reduced transistor count and utilizing naturally commutated thyristors with simple commutation," *In Proceedings of 22nd IEEE Int. Sym. on Power Electronics, Electrical Drives, Automation and Motion, SPEEDAM*, Iscia, Italy, 18-20, June 2014.
[16] Zhang D, Datta R, Rockhill A, et al. "The modular embedded multilevel converter: A voltage source converter with IGBTs and thyristors," *2015 IEEE Energy Conversion Congress and Exposition ECCE*, pp. 1-8, 2015.

Dezhi Chen received the Ph.D. degree in electrical engineering from Shenyang University of Technology, Shenyang, China, in 2014. From 2014 to 2015, he was a post-doctoral fellow in Hanyang University, Korea. He is currently an Assistant Professor with the School of Electrical Engineering, Shenyang University of Technology, Shenyang, China. His research interests include design and analysis of power transformers and special electric machines.

Wenliang Zhao received the B.S. degree in control science and engineering from Harbin Institute of Technology, China, in 2011, and the Ph.D. degree in electronic systems engineering from Hanyang University, Korea, in 2015. From 2015 to 2016, he was a post-doctoral fellow in Hanyang University, Korea. He is currently a Research Professor with the School of Electrical Engineering, Shandong University, Jinan, China. His research interests include design and analysis of electrical machines and power converters.

Byung-il Kwon was born in 1956. He received the B.S. and M.S. degrees in electrical engineering from Hanyang University, Ansan, Korea, and the Ph.D. degree in electrical engineering from the University of Tokyo, Tokyo, Japan, in 1989. He was a Visiting Researcher with the Faculty of Science and Engineering Laboratory, University of Waseda, Tokyo, from 1989 to 2000, a Researcher with the Toshiba System Laboratory in 1990, a Senior Researcher with the Institute of Machinery and Materials Magnetic Train Business in 1991, and a Visiting Professor with the University of Wisconsin-Madison, from 2001 to 2002. He is currently a Professor at Hanyang University. His research interests are design and control of electric machines.